JOURNAL INDIAN ASSOCIATION OF SEDIMENTOLOGISTS ISSN NO 2582 – 2020
Vol. 43, Issue I, 2026, pp. 53 – 63

Origin and Depositional Environment of Elongated Nodules Associated with the Bhander Limestone of the Vindhyan Supergroup around Rewa, Central India: Constraints from Mode of Occurrence, Optical Microscopy and Stable Carbon and Oxygen Isotopic Compositions

D. P. Dubey[1], Yamuna Singh[2*] and Pravin Tiwari[1]
[1]Pradhanmantri College of Excellence, Government Model Science College, Rewa – 486001, Madhya Pradesh
[2]Centre for Earth, Ocean and Atmospheric Sciences, University of Hyderabad, Gachibowli, Hyderabad – 500 046

ARTICLE INFO

KEYWORDS:

Nodules, Organic material;

$\delta^{13}C$;

$\delta^{18}O$;

Dark grey Bhander Limestone;

Freshwater diagenetic environment;

Vindhyan Supergroup;

Rewa;

Central India;

ABSTRACT

The results of investigations on nodules hosted in dark grey Bhander Limestone of the Vindhyan Supergroup from the Rewa area, Central India, are presented. The nodules are either exposed on the surface of the limestone bed or covered by a calcareous layer, making the surface uneven. The material forming nodules is harder than the host limestone. The majority of the nodules are elongated (<4 cm to 2.23 m long) and broader on one side and tapering on the other side. When broken, many calcareous nodules revealed dark scaly organic material in their centre, which, in some cases, changed into black organic material, imparting black color to the host limestone. Optical microscopy revealed the presence of elongated organic materials and segmented, including indeterminate, forms within the nodules. It is interpreted that the scaly material formed a nucleus for the precipitation, and the decomposing organic material provided local chemical conditions in the pore waters, which favoured precipitation of calcium carbonate ($CaCO_3$) following the elongated shape of the organic material. Development of large-scale pits and pores on the limestone surface may be chitinous material, which is a fibrous organic substance known from most arthropods and many invertebrates, and also known to survive over hundreds of millions of years. It is likely that chitinous material on small pits and pores on the limestone surface was later hardened by calcium carbonate precipitation. The $\delta^{13}C$ (proxy of organic matter) values of nodules also indicate depletion of ^{13}C, which is consistent with the influence of the organic-rich matter sources. This interpretation is further supported by the presence of eurypterid and trilobitid impressions in the study area. Chertification of some calcareous nodules is due to occasional precipitation of silica. Significantly, carbonaceous megafossils from the Bhander Group are known from other areas also, and the investigated nodules are from the youngest Bhander Group of the Vindhyan Supergroup. The covariance plots ($\delta^{13}C$-$\delta^{18}O$), depleted carbon and oxygen isotopes ($\delta^{13}C$, $\delta^{18}O$), palaeosalinity and palaeotemperature collectively reveal formation of nodules in a supergene freshwater diagenetic environment under very shallow burial depth.

INTRODUCTION

The nodules are essentially known as small lumps of an assemblage of one or more minerals having compositions generally distinct from their host sedimentary rocks (Neuendorf et al., 2005). In this regard, nodules of pyrite in coal, chert in limestone and phosphorite in marine shale are commonly cited as the best examples. The nodules often lack internal structures and develop in sedimentary rocks during post-depositional chemical activity within the sediments (Neuendorf et al., 2005; Boggs, 2009). Those minerals which generally form nodules are calcite, chert,

***Corresponding Author**
Email: yamunasingh1957@gmail.com
DOI: https://doi.org/10.51710/jias.v43iI.460
Received 27 March 2026; Received in revised form 11 May 2026; Accepted 13 Mayne 2026
Available online 30 June 2026

Table 1: General lithostratigraphic succession of the Upper Vindhyan sediments (After Salujha, 1982, Table 1) and lithostratigraphic succession of the Rewa area (After Singh and Dubey, 1990).

General Lithostartigraphy		Lithostartigraphy of Rewa area (thickness in m)
BHANDER GROUP (Thickness 1000 meters)	Upper Bhander Sandstone	
	Sirbu Shale	Sirbu Shale (5 m)
	Lower Bhander Sandstone	
	Bhnader Limestone	Bhnader Limestone (25 m)
	Ganurgarh Shale	Ganurgarh Shale (25 m)
REWA GROUP (Thickness 2000 meters)	Upper Rewa Sandstone	Rewa Sandstone (125 m)
	Jhiri Shale	Rewa Shale (20 m)
	Lower Rewa Sandstone	
	Panna Shale	

apatite, anhydrite and pyrite (Neuendorf et al., 2005; Boggs, 2009). The nodules are also referred to as metallic concretions of manganese, cobalt, iron, and nickel, including phosphorite, on the seafloor. Such nodules form resources for multiple critical metal deposits from the surface of the ocean floor beds (Li et al., 2023; Ren et al., 2023). This paper describes elongated calcareous and cherty nodules from dark-grey limestone of the Bhander Group (Upper Vindhyan) of the Vindhyan Supergroup developed around Rewa (Survey of India Toposheet No. 63H; $24^0 30'$ - $24^0 40'$; $81^0 10'$ - $81^0 25'$) in Central India; and, on the basis of mode of occurrence, optical microscopy and stable carbon and oxygen isotopic compositions, genesis and depositional environment of nodules are constrained.

LITHOSTRATIGRAPHY

The Rewa area forms a part of the vast Vindhyan Supergroup, which covers an area of about 120000 km^2, with a sediment thickness of more than 4500 meters. The Vindhyan Supergroup is divided into four Groups of unequal thickness in ascending order, namely, Semri-, Kaimur-, Rewa- and Bhander-Group (Table 1). Out of these four Groups, the Semri Group (Lower Vindhyan) and Bhander Group have well-developed limestone along with sandstone and shale, whereas the Kaimur Group and the Rewa Group are dominated by sandstone with some shale sequences (Table 1). The reported ages of the Semri-, Kaimur-, Rewa- and Bhander-Group are 1.7-1.6 Ga, <1.2 Ga, ~1.1 Ga (?) and 1.1-0.7 Ga, respectively (George et al., 2025).

The Rewa Sandstone, Ganurgarh Shale and Bhander Limestone show extensive development around Rewa, whereas Sirbu Shale is localized in a hillock near Bela (Fig. 1). Limestones exposed around Rewa are stromatolitic and non-stromatolitic, well-bedded to massive and hummocky-type, and vary in colors from dirty white, light pink, light grey to dark grey, with or without stromatolites of mainly Collenia Group (Dubey, 1981; Singh and Dubey, 1990; Dubey et al., 2009). Microfacies analysis revealed that the limestones of the area are mainly micritic, oomic-sparitic, with sparites of aggradational neomorphic origin (Singh and Dubey, 1993, 1998, 1999). In some limestones, allochems, ooids, peloids and intraclasts are also present (Singh and Dubey, 1998). The limestones were deposited under a shallow marine tidal environment (Singh and Dubey, 1993, 1998, 1999). The presence of specks of pyrite (FeS_2) in dark grey limestone also suggests the prevalence of occasional reducing conditions in the depositional basin.

The limestone forms a slightly raised, flattened topographic high above ground, spread over an area of about 10 km^2, where the local APS University Rewa has its campus. The University is built on an east-west trending low-lying ridge hiding well-developed bioherms of algal origin (Tiwari and Dubey, 2004). The longest exhumed bioherm is 4.0 meters long, 3.0 meters wide and 2.0 meters high (Fig. 2a). The eastern part of the area is occupied by bioherms of different lengths, widths and heights. About a kilometer west of the biohermal field, well-bedded and massive hummocky

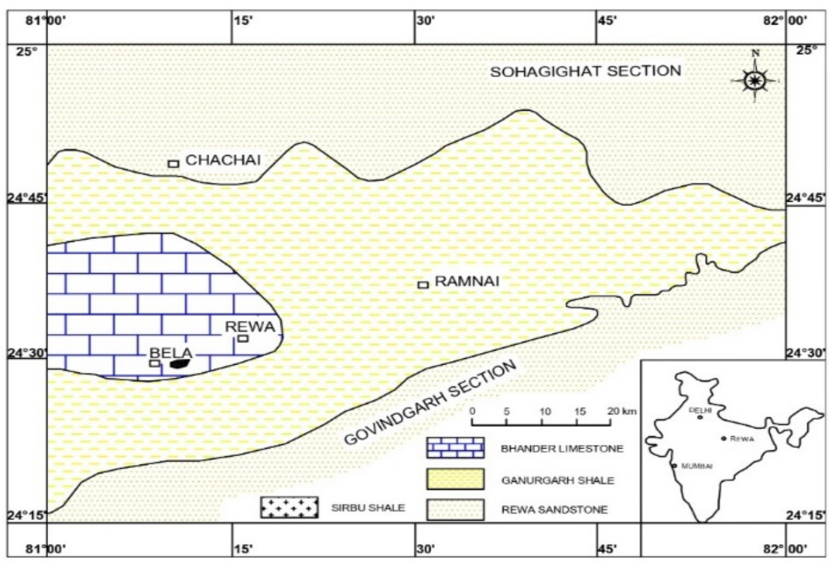

Fig. 1. Geological map of the Rewa area (Redrawn and modified from Singh and Dubey, 1990).

dark grey non-stromatolitic limestones are exposed. Elongated nodules occur within the dark grey limestone with a distinct border (Fig. 2b). Also, the surface of the limestone

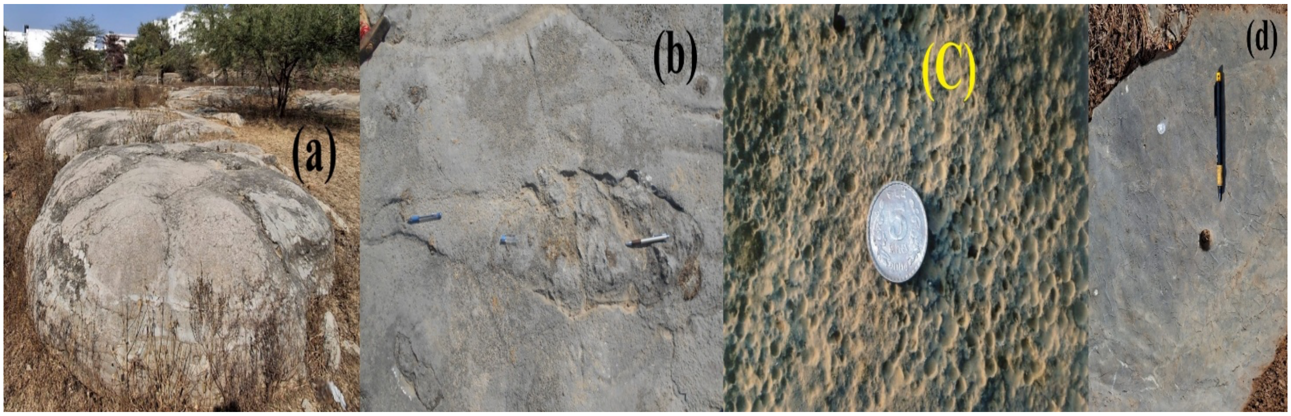

Fig. 2. **(a)** Field photographs of exhumed bioherms of algal origin. **(b)** Elongated and segmented calcareous nodule embedded in dark grey limestone. Note that the nodule surface is different from its host limestone. **(c)** Closely-spaced pitting on the surface of the dark grey limestone. **(d)** Dark grey limestone displaying profuse track and trail marks.

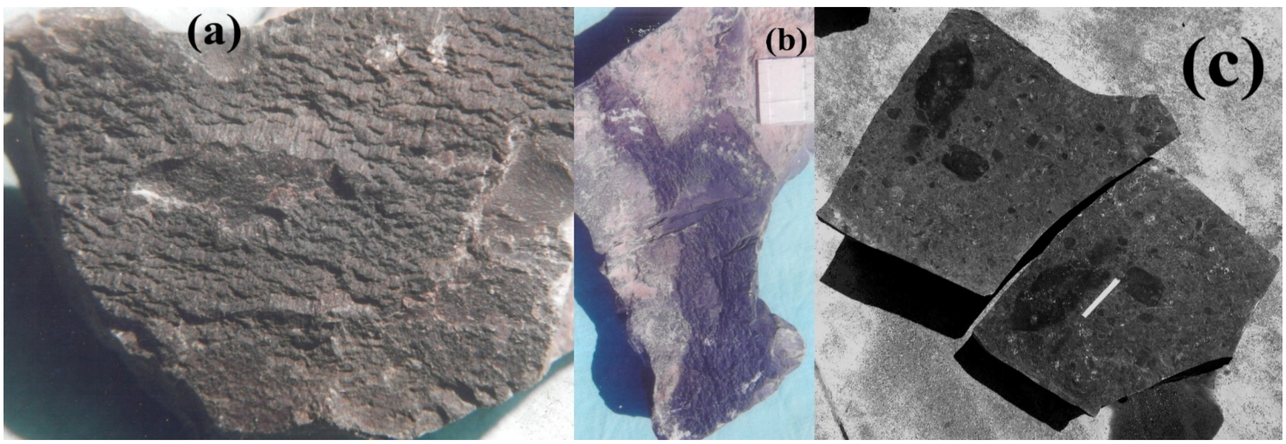

Fig. 3. **(a)** Calcareous nodules adorned with small to medium sized grains and distinct platy structure. **(b)** Dark scaly material formed by precipitation during decomposing organic material, as revealed on breaking of few nodules. **(c)** Carbonized compression, which is broader interiorly and narrowing posteriorly.

displays closely-spaced pits, unlike rain prints (Fig. 2c). Track and trail marks are also profusely seen (Fig. 2d). A few nodules have two distinct parts, one platy /scaly (Fig. 3a, 3b) and the other without it. At places, carbonized compression is clearly observed, with broader anterior and narrower posterior (Fig. 3c). Another interesting aspect of the dark grey limestone, which hosts nodules, is that, when struck with a hammer, it emits fetid odour. Pettijohn (1984) believes that such odour may be due to the presence of hydrocarbons in limestone. All the investigated nodules are from the dark grey non-stromatolitic limestone.

CHARACTERISTICS OF THE NODULES

Field Characteristics

The investigated nodules in the area do not indicate any set pattern of distribution. They are randomly oriented within the host limestone. The nodules are either exposed on the surface of the limestone bed or covered by a calcareous layer, making the surface uneven (Fig. 4a, 4b, 4c, 4d). In fact, the limestone that hosts nodules shows a wavy surface. The material forming nodules is harder than the host limestone. Also, nodules generally have a composition different from the host rock. Nodules appeared after removing a 20 to 30 cm thick upper layer of limestone (Fig. 4b). Sometimes, in bedded limestone, rectangular joints on the surface indicated the presence of elongated nodules. Pitted limestone surfaces also helped in locating nodules. The presence of calcite veins on the limestone surface also indicated the presence of nodules (Fig. 4d). Due to these features, nodules are distinctly visible in the field. The investigated nodules range in length from less than 4 cm to 2.23 meters. Although shapes and patterns of distribution of nodules within the host rock are highly variable, but majority of the nodules, whether calcareous or cherty, are elongated and broader on one end and tapering on the other end. Brief details of the individual nodules are presented separately (Table 2), along with most of the corresponding field photographs (Fig. 4e, f, g, h, i, j, k, l, m).

Optical Microscopic Characteristics

Thin sections of a few nodules were prepared and examined under an optical microscope. The study of micro-

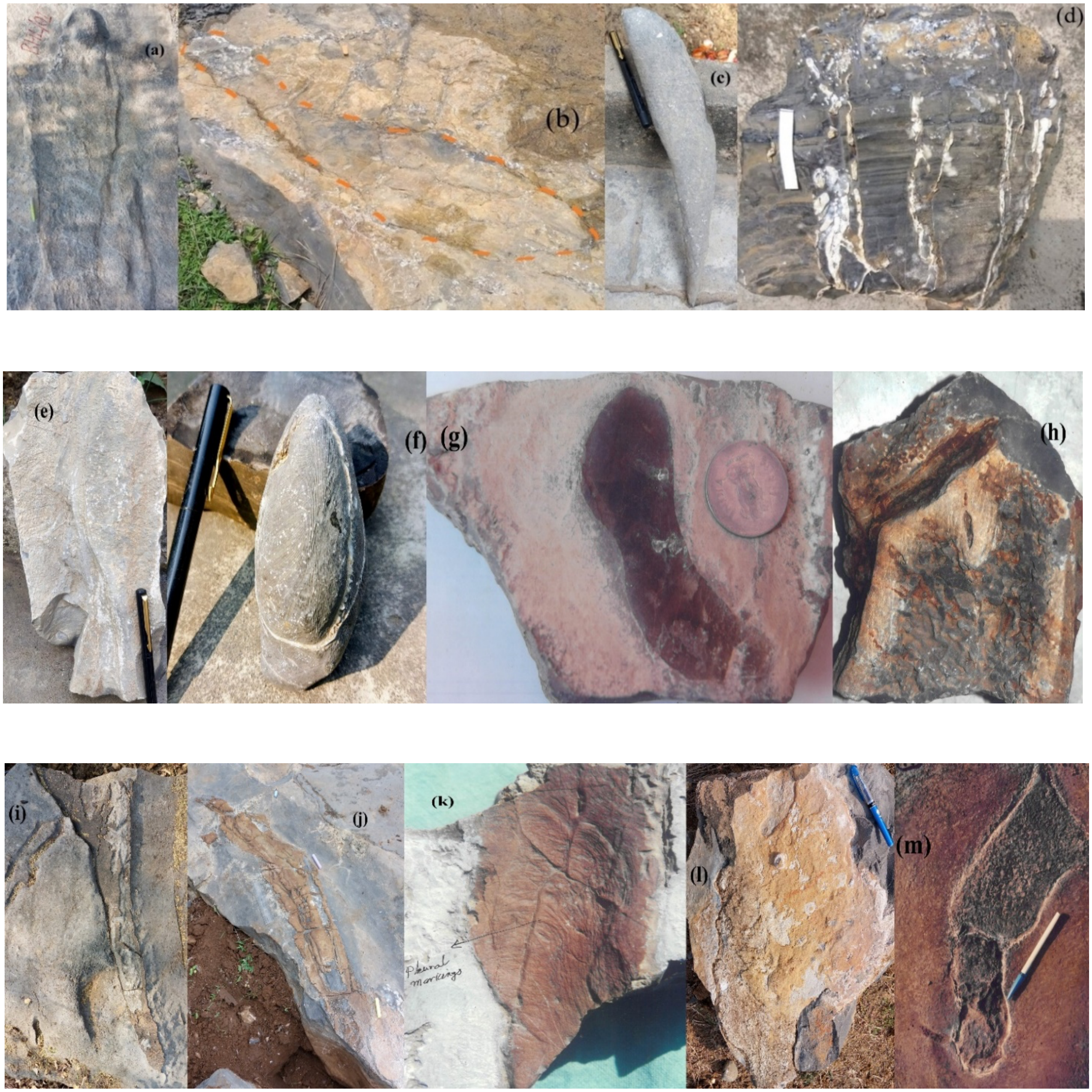

Fig. 4. **(a)** Elongated nodule showing distinct transverse marking lines. Note lower part is very thin. **(b)** Elongated nodule obtained after removing 25cm thick layer of limestone. **(c)** Elongated nodule with rough surface due to small grains. It appears nodule is grown over some organic material present inside. **(d)** Calcareous nodule displaying development of two long platy structures on both sides - broader in the upper part with tapering downward. Also, note development of calcite veins in the nodule. **(e)** Calcareous nodule obtained from dark grey limestone after removing 5cm thick limestone layer. **(f)** Nodule separated from the dark grey limestone. **(g)** Brownish nodule with nearly smooth surface and variable width. The upper and lower parts of the nodule are rounded. **(h)** Calcareous nodule with broadening on the upper side and narrow rounded shape on the lower part. A linear groove also bisects the nodule. **(i)** Silicified cherty nodule with small grains on the surface. Thick transverse lines are also developed. **(j)** Siliceous nodule with upward pointed upper part that is detached from the main body. Transverse lines and grains are also seen. **(k)** A relatively thin and slightly depressed cherty nodule, with two distinct parts. Note more distinct markings on right hand side. **(l)** Silicified nodule having broad upper part, which is incomplete due to breaking. **(m)** A nodule with slightly raised upper part. Also, note that its lower part is thin surface with pits.

Table 2: Characteristics features of the investigated nodules developed in the Rewa area.

Nodule No.	Composition of Nodule	Host Rock of Nodule	Colour of Nodule	Dimension			Morphology of Nodule	Fig.
				Max. Length	Max. Width	Min. Width		
1	Calcareous	Dark grey limestone	Dirty grey	2.23m	33cm	01mm	Elongated nodule adorned with granules, which are not present in the host rock. Nodule is cut by traverse lines. Its lower part is very thin.	4(a)
2	Calcareous	Dark grey limestone	Pale yellow	1.92m	35cm	02mm	The elongated nodule obtained after removing 25cm thick layer of limestone. Small grains seen on the surface. Spaced traverse lines cut the nodule. Its lower part is thin. This nodule is part of the host rock in the field.	4(b)
3	Calcareous	Host rock was dark grey limestone now separated	Grey	31cm	04cm	01cm	The elongated nodule with rough surface due to small grains. Transverse lines present on both sides. Vertical lines seen on the right and left sides. It appears nodule is grown over some organic material present inside.	4(c)
4	Calcareous	Separated and collected from dark grey limestone	Dark grey	14cm	11cm	07cm	Two distinct parts in the nodule. The upper part is sub rounded without plates. The lower part has six plates of variable width. Two long platy structures developed on both sides. Broader in the upper part but thinning downward, white calcite veins effect the nodule.	4(d)
5	Calcareous	Obtained from dark grey limestone after removing 5cm thick limestone layer	Light pink	26cm	Upper width 03cm middle 09cm	02cm	The body is having closely spaced transverse lines not seen in the surrounding host rock. Three triangular structures developed on the left side of the nodule.	4(e)
6	Calcareous	Separated from the dark grey limestone	Dark grey	14cm	06cm	05cm upper, 4cm lower	This is only slightly elongated; the lower and upper parts are slightly flattened. The middle part is thick. Radiating etch marks on the surface after treating with dilute HCL. White calcite veins present suggesting presence of same foreign body inside.	4(f)
7	Calcareous	Recovered from dark grey limestone	Light brown	8.5cm	3.5cm	1.8cm to 05cm	This brownish nodule has nearly smooth surface. It has variable width. The upper and lower parts are rounded.	4(g)
8	Calcareous	Dark grey limestone	Dirty white	5cm	3cm groove	3cm long, 2cm width	This calcareous nodule form is broader on the upper side and narrow rounded on the lower part. A linear groove bisects the nodule. The nodule in the upper part is attached with a broad linear groove. This nodule resembles the figure of arthropod hypostome, as shown by Woods (1958) and Shrock and Twenhofel (1987). The area below nodule is showing pits and irregular ridges.	4(h)
9	Siliceous (Cherty)	Dark grey limestone	Dirty white	50cm	15cm	5cm broken not complete	The nodule has small grains on the surface. In the middle part of the nodule thick transverse lines are developed. On both sides of the nodule, dark grey host limestone is visible.	4(i)

10	Siliceous (Cherty)	Dark grey limestone	Nearly black	90cm	15cm	5cm	The upper part of the nodule is pointed upward. It is detached from the main body. The nodule is gradually thinning on one side. Grains are seen on the surface. Transverse line (cracks) cut the nodule. The host limestone is profusely pitted.	4(j)
11	Siliceous (Cherty)	Dark grey limestone	Pale yellow	10cm	04cm	03cm	The nodule is not very thick and slightly depressed. It has two distinct parts. The upper parts are nearly plain with notch in the middle. The lower part is 10 cm long and 4 cm wide, some marking resembling pleurae of arthropods are seen on the both sides of a central line. Markings are more distinct on right hand side. Length of marking is 3.4 cm. The nodule is broader on upper side and thinner and bent downward.	4(k)
12	Siliceous (Cherty)	Dark grey limestone	Black spots of grey	60cm	15cm	4cm	The elongated nodule is exposed on the surface of a dark grey limestone. The upper part is broad, but incomplete due to breaking. The nodules thickness is slightly less in the lower part. Transverse cracks cut the nodule without affecting host limestone. The host limestone has closely spaced pits. The under surface of the nodule is blackish with un-replaced part of the calcareous nodule.	4(l)
13	Calcareous	Dark grey limestone	Brownish	22cm	6cm	5cm	The nodule is slightly raised in the upper part. Lower part is thin surface with pits. A deep notch is also seen.	4(m)

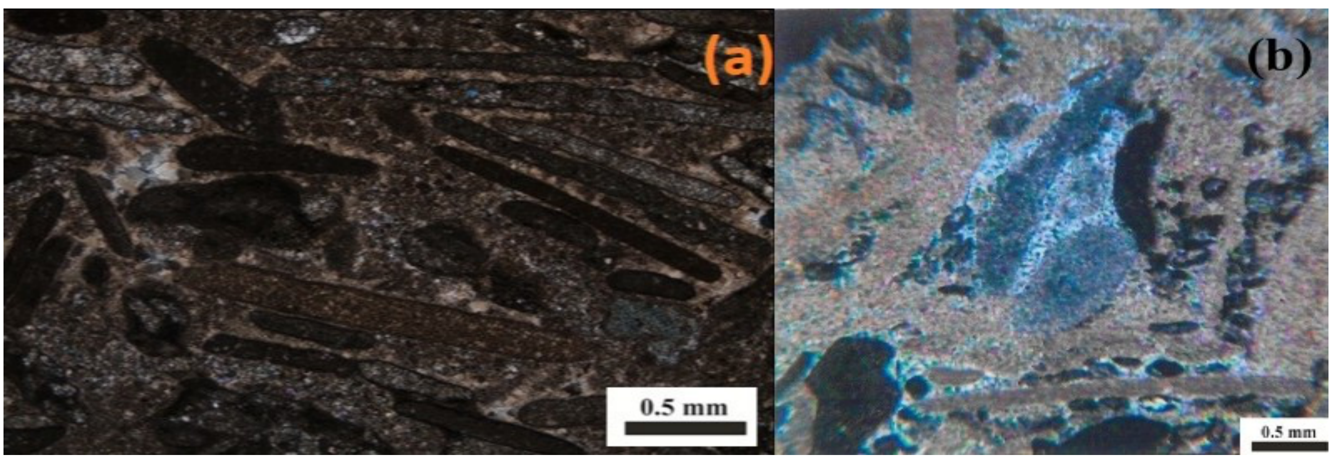

Fig. 5. Microphotographs of calcareous nodules of the Rewa showing **(a)** Elongated organic material and **(b)** Segmented organic material. Some indeterminate forms are also present

organic materials (Fig. 5a). In addition, the organic materials also revealed clearly segmented forms within the nodules (Fig. 5b). Some indeterminate forms are also present.

Stable Carbon and Oxygen Isotopic Characteristics

A total of 9 nodules were analyzed at CSIR-National Geophysical Research Institute, Hyderabad, for their stable carbon and oxygen isotopic compositions

Table 3: Stable carbon and oxygen isotopic compositions of the investigated calcareous nodules associated with the dark grey limestone of the Rewa area.

Identifier I	Analysis	δ^{13}C (in ‰; with reference to value in VPDB)	δ^{18}O (in ‰; with reference to value in VSMOW)	Palaeosalinity (Z)	Palaeotemperature (T^0C)
BUL – 10 (REP)	6763	-5.00	-23.84	-	-
BUL – 05 (REP)	6763	-5.05	-24.62	-	-
BUL – 12	6763	-5.45	-26.71	102.8	130.5
BUL – 11	6763	-4.21	-23.44	107.0	115.7
BUL – 10	6763	-5.01	-23.83	105.1	117.5
BUL – 09	6763	-5.06	-21.09	106.4	105.0
BUL – 08	6763	-4.77	-22.28	106.4	110.4
BUL – 07	6763	-3.72	-21.92	108.7	108.8
BUL – 06	6763	-4.87	-24.19	105.3	119.1
BUL – 05	6763	-5.11	-24.67	104.5	121.3
BUL – 04	6763	-4.48	-24.15	106.1	118.9

(Table 3; Devleena Mani Tiwari, Analyst). Also, analysis of two samples, namely, BUL-10 (REP) and BUL-05 (REP), was repeated (Table 3). The analysis was done using an isotopic ratio mass spectrometer (IRMS). The data of stable carbon isotopic compositions of nodules are expressed in parts per thousand (‰) of δ^{13}C, which is a well-known proxy of organic matter. The range of δ^{13}C values (a ratio that compares the ^{13}C to ^{12}C ratio of a sample to a standard, the Vienna Pee Dee Belemnite – VPDB, and the values indicate the relative depletion of ^{13}C with reference to the VPDB) is narrow, ranging from -3.72‰ to -5.45‰ (Fig. 6). The data of stable oxygen isotopic compositions of nodules are also

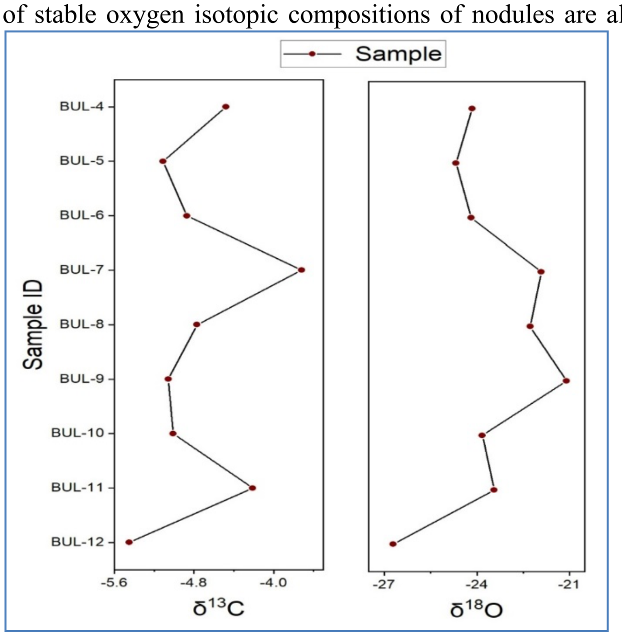

Fig. 6. Variation in the range of δ^{13}C and δ^{18}O values of the investigated calcareous nodules.

expressed in parts per thousand (‰) of δ^{18}O. The range of δ^{18}O values (a ratio that compares the ^{18}O to ^{16}O ratio of a sample to a standard, the Vienna Standard Mean Ocean Water – VSMOW, and the values indicate the depletion of ^{18}O with reference to the VSMOW) is also narrow, and varies from -21.09‰ to -26.71‰ (Fig. 6; Table 3; Devleena Mani Tiwari; Analyst). The plots of δ^{13}C-δ^{18}O fall in the field for a supergene freshwater diagenetic environment (Fig. 7; Fields after Liu Xiaofeng et al., 2023). The scatter plots between δ^{13}C and δ^{18}O reveal a notable covariation between the two, the fitting equation being y = 1.6*x + -16, with a coefficient of determination 0.254 (Fig. 8).

DISCUSSION

Origin of Nodules

Localization of nodules in the dark grey limestone of the Rewa University area is conspicuous (Fig. 2b). When broken, many calcareous nodules revealed dark scaly organic material in their centre (Fig.3b). The scaly material in some cases changed into black organic material. It is for this that the dark grey limestone of the Rewa University area has a black color. For a particular mineral to be precipitated, the pore water within the sediments must be supersaturated with constituent ions. In addition, acidity, alkalinity (pH) and oxidation-reduction (Eh) potential must also be appropriate (Collinson and Thompson, 1989). Therefore, the only possible explanation is that something in the host dark grey limestone itself caused the chemical condition to be suitable for segregation of calcium carbonate ($CaCO_3$) locally at places, and not everywhere. Interestingly, the investigated nodules do not follow bedding. Also, there is no possibility of rootlets controlling nodule growth. So, the only possibility is that the available organic material provided a conducive environment for the development of nodules. The role of scaly organic material (Fig. 3a, b), which is present in the host limestone, seems most important in this regard. It is therefore interpreted that the scaly material (Fig. 3a, b) formed a nucleus for the precipitation, and the decomposing organic material provided local chemical conditions in the pore waters, which favoured precipitation of calcium carbonate following the elongated and segmented shape of the organic material (Fig. 3c; 5a, b), and thereby elongated calcareous nodules (Table 2). Large-scale development of pits and pores on the limestone surface (Fig. 2c) may be chitinous material in these nodules. Chitin is a complex organic substance that is present in most arthropods and many invertebrates (Bailey et al., 2025). It has a fibrous structure commonly adorned with surface pits, spines and tiny perforations. Further, chitin is also known to survive over hundreds of millions of years (Bailey et al., 2025). It is possible that the limestone surface with small pits and pores (Fig. 2c) may be the place of chitin, which was later on hardened by calcium carbonate ($CaCO_3$) as suggested by Shrock and Twenhofel (1987). The range of $\delta^{13}C$ values of nodules, being from -3.72‰ to -5.45‰ (Table 3; Fig. 6), is also consistent with the influence of the organic-rich matter sources (Liu Xiaofeng et al., 2023). This interpretation is further supported by the eurypterid and trilobitid impressions in the study area (Dubey, 1982). Occasional chertification (Fig. 4j, k, l) of some calcareous nodular forms is attributed to precipitation of silica (Dubey et al., 2009; Boggs, 2009; Ali et al., 2026). It is imperative to mention that carbonaceous megafossils from the Bhander Group are known from other areas also (Kumar and Shrivastava, 2003), and the investigated nodules are from the youngest Bhander Group of the Vindhyan Supergroup. Furthermore, even from the lower Vindhyan rocks, arthropod impressions have been reported (Tandon and Kumar, 1977a, b). Preservation of trace fossils, pseudo-fossils, ichnofossils, microfossils, and mega-fossils is also reported from different parts, involving both Lower and Upper Vindhyans (Table 1), of the Vindhyan Basin (Mathur, 1983; Rai and Gautam, 1988; Kumar, 1995; Venkatachala et al., 1996; Choudhuri et al., 2020).

Depositional Environment

The sensitivity of oxygen isotopes is known to change during later stages of sedimentation (Xiao et al., 1997; Shields, 2010). The significant decrease in $\delta^{18}O$ value is known when exchange takes place during atmospheric precipitation or hydrothermal fluids (Xiao et al., 1997; Shields, 2010). The $\delta^{18}O$ values of -26.71 to -21.09 suggest that the investigated nodule samples are depleted in ^{18}O with reference to the value in the standard (VSMOW) by -26.71 to -21.09 parts per thousand (Table 3). Such a variation reflects the gradual depletion of ^{18}O in an air mass as it leaves the ocean and moves to the continent (Taylor, 1979). The calculated values of the palaeosalinity (Z) range between 102.8 and 108.7 (Table 3). Based on the values of Z, a depositional environment has been postulated by earlier researchers (Keith and Weber, 1964). It is stated that when a carbonate rock has a value of Z >120, it formed under marine sedimentation, whereas when the value of Z is <120, its formation took place under freshwater conditions (Keith and Weber, 1964). All the investigated nodules have Z values (104.5 to 108.7) <120, suggesting that they formed under freshwater diagenetic conditions. The plots of $\delta^{13}C$-$\delta^{18}O$ of nodules also support the formation of nodules under a supergene freshwater digenetic environment (Fig. 7; Fields after Liu Xiaofeng et al., 2023). Furthermore, a notable trend of co-variation in between $\delta^{13}C$-$\delta^{18}O$ (Fig. 8) also supports the meteoric water mix for a single generation of carbonate cement (Allan and Mathews, 1982). Notably, the covariation is known to be linked with the mixing of meteoric water and seawater, where meteoric water is depleted in ^{18}O relative to its seawater, and once it has moved through organic material, it also gets enriched in ^{12}C (Allan and Mathews, 1982). Thus, it is likely that within the regional framework of the shallow marine sedimentation (Singh and Dubey, 1993, 1998, 1999),

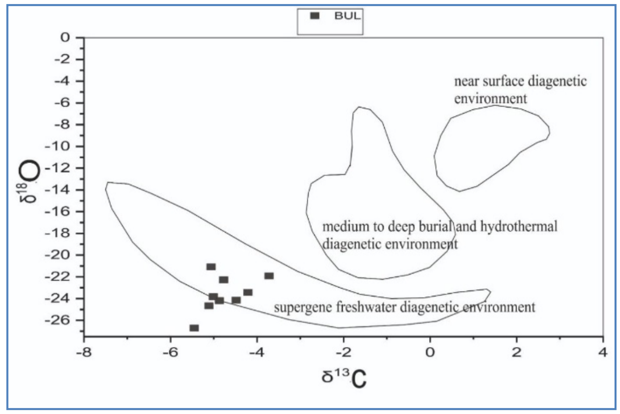

Fig. 7. Plots of $\delta^{13}C$-$\delta^{18}O$ of the investigated calcareous nodules (Fields after Liu Xiaofeng et al., 2023).

locally freshwater mixing conditions prevailed where nodules formation took place. Interestingly, the values of calculated palaeotemperature (T) of the nodules come to be in the range of 105 to 121⁰C, with an average of 115⁰C

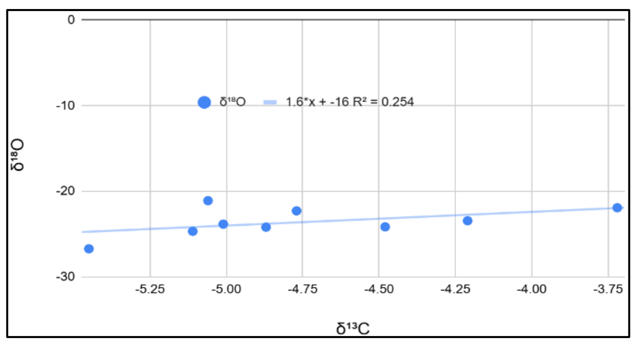

Fig. 8. Scatter plots of $\delta^{13}C$ and $\delta^{18}O$.

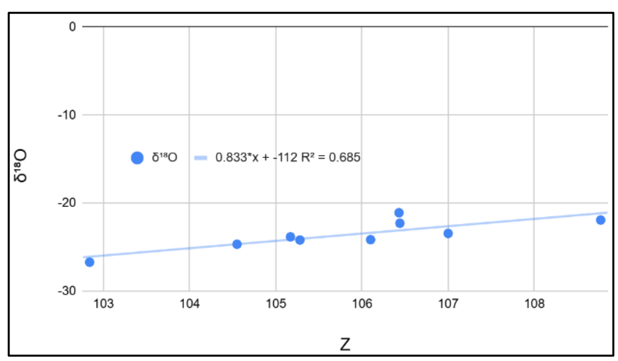

Fig. 9. Scatter plots of palaeosalinity (Z) and $\delta^{18}O$

(excluding one value of 130.5, Table 3). Such an elevated palaeotemperature (T) is again expected to be linked with the formation of nodules under very shallow water conditions, where palaeotemperature was ~115^0C due to very shallow burial depth. A marked covariation of palaeosalinity (Z) and δ^{18}O is also brought out by the scatter plots in between the two, the fitting equation being y = 0.833*x + -112, with a coefficient of determination 0.685 (Fig. 9). It is consistent with the known fact that the palaeosalinity (Z) is a controlling factor in limestone formation (Xie et al., 2009). Interestingly, still better covariation is revealed by the scatter plots of palaeosalinity (Z) and δ^{13}C, the fitting equation being y = 0.286*x + -35, with a coefficient of determination 0.813 (Fig. 10). Both the scatter plots (Figs. 9 and 10) clearly suggest the significant role of palaeosalinity (Z) in δ^{13}C-δ^{18}O values and, thereby in the deposition of limestone hosting the investigated nodules.

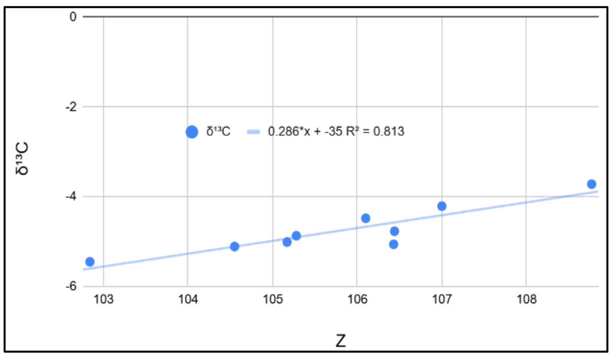

Fig. 10 Scatter plots of palaeosalinity (Z) and δ^{13}C.

CONCLUSIONS

1. The investigated nodules are mostly elongated (<4 cm to 2.23 m long), tapering type, and contain dark scaly, elongated and segmented organic materials within them.

2. It is likely that the scaly material formed a nucleus for the precipitation, whereas the decomposing organic material provided local chemical conditions in the pore waters, which favoured precipitation of calcium carbonate ($CaCO_3$) following the elongated shape of the organic material.

3. Development of large-scale pits and pores on the limestone surface may be chitinous material, which was hardened later by calcium carbonate precipitation.

4. The depletion of δ^{13}C values of nodules is also consistent with the influence of the organic-rich matter sources in the genesis of nodules.

5. Chertification of some calcareous nodules is attributed to occasional precipitation of silica.

6. The results of studies strongly suggest the presence of both micro and mega-fossils, and therefore, comprehensive field and laboratory investigations are necessary to explore this potential of the Rewa area.

7. The covariance plots (δ^{13}C-δ^{18}O), depleted isotopic compositions (δ ^{13}C, ^{18}O), palaeosalinity and palaeotemperature collectively reveal formation of nodules in a supergene freshwater digenetic environment under very shallow burial depth.

ACKNOWLEDGEMENTS

The authors express their sincere gratitude to Prof. (Dr.) S.K. Tandon and Dr. Suchna Taral for their valuable technical input, guidance and suggestions; to Dr. Devleena Mani Tiwari, CSIR-National Geophysical Research Institute, Hyderabad (Presently with University of Hyderabad, Gachibowli, Hyderabad) for providing 'C' and 'O' isotopic data on the investigated nodules; to Prof. Milind Herlekar, Convener, 41st Annual Convention of the IAS and National Conference on Sedimentology, held during 19-21 January 2026, at Department of Geology, Savitribai Phule Pune University, Pune-411007 for providing opportunity to present this paper; to the two anonymous reviewers for their insightful review comments and useful suggestions which improved manuscript; to Prof. G.N. Nayak and Dr. J.S. Armstrong-Altrin present and immediate past Editor-in-Chief, for useful editorial comments and efficient handling of the manuscript; and to, for invitation to contribute paper for Journal of the Indian Association of Sedimentologists.

CREDIT ATHORSHIP CONTRIBUTION STATEMENT

D P. Dubey - Conceptualization, Field work, Methodology, Investigation, Visualization, Photography, Interpretation, Writing – original draft, review and editing, Revision, Validation, Supervision.

Yamuna Singh: Field work, Conceptualization, Methodology, Isotopic data acquisition, Data processing, Data interpretation, Writing – original draft, review and editing, Revision, Validation;

Pravin Tiwari: Field work, Methodology, Photography, Data interpretation, Writing – original draft, review and editing.

FUNDING:

This work did not receive any funding from any source.

DATA AVAILABILITY:

Data related to this work are presented in paper.

DECLARATION OF CONFLICTING INTEREST:

The authors declare that there is no known conflict of interest.

REFERENCES

Ali, Z.Z., Asaad, I.S., Al-Juboury, A.I., Akkoca, D.B. (2026). Petrography, mineralogy and geochemistry of the chert nodules in the Middle-Late Eocene Pila Spi Formation, high folded zone, northern Iraq; Journal of African Earth Sciences,https://doi.org/10.1016/j.jafrearsci.2026.106056

Allan, J.R. and Matthews, R.K. (1982), Isotope signatures associated with early meteoric diagenesis; Sedimentology, v. 29, p. 797-817.

Bailey, E., Tsurkan, M., Nowacki, K., Jesionowski, T., Ehrlich, H. (2025). Evidence for surviving chitin in Cambrian trilobites from the Carrara Formation, Western North America; PALAIOS, v. 40 (12), p. 379-387. https://doi.org/10.2110/palo.2024.025.

Boggs, S. Jr. (2009). Petrology of Sedimentary Rocks; Cambridge University Press, Cambridge, United Kingdom, 600p.

Choudhuri A., Banerjee, S., Sarkar, S. (2020). A review of biotic signatures within the Precambrian Vindhyan Supergroup: Implications on evolution of microbial and metazoan life on earth; Journal of Mineralogical and Petrological Sciences, v.115, p. 162-174.

Collinson, J.D. and Thompson, D.B. (1989), Sedimentary structures Unwin Gyman Ltd U.K., 207p.

Dubey, D.P. (1981). Sedimentological study of some selected sections of the Vindhyan Supergroup around Rewa, (M.P.); Unpublished PhD Thesis, A.P.S. University, Rewa (M.P.).

Dubey, D.P. (1982). A preliminary note on the eurypterid and trilobitid remains from the upper Vindhyan Rocks around Rewa, Madhya Pradesh; In: Current Trends in Geology, v.7, p. 63-78, Proc. IV Indian Geological Congress. Today and Tomorrow's Printers and Publishers, New Delhi.

Dubey, D.P., Tiwari, R.N., Shrivastava, R.K. (2009). Petrography of chert nodules from the Bhander Limestone Formation, Rewa district, Madhya Pradesh; Gondwana Geological Magazine, v. 24 (2), p. 157-160.

George, B.G., Ray, J.S., Mahala, M.K., Dev, J.A., Thomson, J.K., Haripriya, J., Alok Kumar (2025). Geochronology of the Vindhyan Supergroup: Implications for the closure of the Proterozoic basins of India; Precambrian Research, v. 422, p. 107790/1-11. https://doi.org/10.1016/j.precamres.2025.107790

Keith, M.L. and Weber, J.N. (1964), Isotopic composition and environmental classification of selected limestones and fossils; Geochim. Cosmochim. Acta, v. 28, p. 1786-1816.

Kumar, S. (1995). Megafossils from the Mesoproterozoic Rohtas Formation (the Vindhyan Supergroup), Katni area, central India; Precambrian Research, v. 72 (3-4), p. 171-184.

Kumar, S. and Shrivastava, P. (2003), Carbonaceous mega fossils from the Neoproterozoic Bhander Group, Central India; Journal of the Palaeontological Society of India, v.48, p. 139-154.

Li, C., Song, W., Sun, Z., Hu, G., Yuan, X, Kao, S. J. (2023). Control on critical metal enrichments in ferromanganese nodules from the Philippine Sea, at water depths of 4400-6000 m; Minerals, v. 13, p. 522. https://doi.org/10.3390/min13040522

Liu Xiaofeng, Hong, Z., Liang, J., Guo, X., Xue, X., Li, S. (2023). Carbon and oxygen isotope characteristics of carbonate rocks in the Mesoproterozoic Jixian System of the Ordos Basin and their implications; Scientific Reports, v. 13, p. 14082. https://doi.org/10.1038/s41598-023-41297-w

Mathur, S.M. (1983). A reappraisal of the trace fossils described by Vredenburg (1908) and Veer (1919) in rocks of the Vindhyan Supergroup; Records of Geological. Survey of. India, v. 113(2), p. 111-113.

Neuendorf, K.K.E., Mehl, J.P., Jackson, J.A. (Editors) (2005). Glossary of Geology, 5th Edition, Alexandria, Virginia, American Geological Institute, 779 p.

Pettijohn, F.J. (1984). Sedimentary Rocks, 3rd Edition CBS Publishers, Delhi.

Rai, V. and Gautam, R. (1998), New occurrence of carbonaceous megafossils from the Meso- to Neoproterozoic horizons of the Vindhyan Supergroup, Kaimur-Katni areas, Madhya Pradesh, India; Geophytology, v. 26, p. 13-25.

Ren, X., Li, H., Yan, S., Li, H., Shi, X. (2023). Hydrogenetic and diagenetic controls on the specific surface area of polymetallic nodules in deep ocean basins; Minerals, v. 13, p. 1431. https://doi.org/10.3390/min13111431

Salujha, S.K. (1982). Palynology of the surface and subsurface Vindhyan sediments; In: K.S. Valdiya, S.B. Bhatia and V.K. Gaur (Eds.), Geology of Vindhyanchal. Hindustan Publishing Corporation, Delhi, p. 113-124.

Shields, G.A. (2010). Neoproterozoic cap carbonates: a critical appraisal of existing models and the plume world hypothesis; Terra Nova, v. 17 (4), p. 299-310.

Shrock, R.R. and Twenhofel, W. (1987), Principles of Invertebrate Palaeontology. Second Edition, CBS Publisher, Delhi.

Singh, Y. and Dubey, D.P. (1990), The stratigraphy and depositional environments of the Vindhyan Sediments in Rewa area, Madhya Pradesh; Geological Survey of India, Spl. Pub. No. 28, p.354-364.

Singh, Y. and Dubey, D.P. (1993), Lithostratigraphy, microfacies and depositional environments of the Proterozoic Bhander Limestone from Central India; In: Jhingran, V. (Ed.) Recent Researches in Sedimentology. Hindustan Pub. Corp., New Delhi, p.130-140.

Singh, Y. and Dubey, D.P. (1998), Petrology of Bhander Limestone of Rewa area, Madhya Pradesh, India; Gondwana Geological Magazine, v.13, p. 21-38.

Singh, Y. and Dubey, D.P. (1999), Nature of cementation and its role in the diagenetic history of Late Proterozoic Bhander Limestone of Rewa area, central India; Journal of Indian Association of Sedimentologists, v.18 (1), p.111-112.

Tandon, S.K. and Kumar, S. (1977a), New fossil finds from the lower Vindhyan rocks (Precambrian of Central India); Current Science, v.46 (6), p. 563.

Tandon, S.K. and Kumar, S. (1977b), Discovery of annelid and arthropod remains from Lower Vindhyan Rocks (Precambrian) of central India; Geophytology, v. 7(1), p. 126-129.

Taylor, H.P. (1979). Oxygen and hydrogen isotope relationships in hydrothermal mineral deposits. In: Barnes H.L. (ed.), Geochemistry of hydrothermal ore deposits, 2nd edition, Wiley, New York, p. 236-277.

Tiwari, R.N. and Dubey, D.P. (2004), Exhumed Bioherms (Patch Reefs) in Bhander Limestone of Rewa Region, Madhya Pradesh. Gondwana Geological Magazine, v.19 (2), p.177-178.

Venkatachala, B.S., Sharma, M., Shukla, M. (1996). Age and life of the Vindhyans; facts and conjectures; Memoir Geological Society of India, v. 36, p. 137-165.

Woods, H. (1958). Invertibrate Palaeontology, Eighth Edition, Cambridge University press, London, U.K.

Xiao, S., Knoll, A.H., Kaufman, A.J., Yin, L.M., Zhang, Y. (1997). Neoproterozoic fossils in Mesoproterozoic rocks? Chemostratigraphic resolution of biostratigraphic conundrum from the North China Platform; Precambrian Research, v. 84 (3**),** p. 197-220.

Xie, X.M., Hu, W.X., Wang, X.L., Qian, Y.X., Zhang, J.T., Cao, J., Li, Q. (2009). Sedimentary sequences in Keping area, Xinjiang: Constraints from carbon and oxygen isotope compositions of Cambrian Ordovician carbonate rocks; Geochimica, v. 38(1), p. 75–88.